



Methods and  
techniques



**Cite this article:** Löptien J, Vesting S, Dobler S, Mohammadi S. 2024 Evaluating the efficacy of protein quantification methods on membrane proteins. *Open Biol.* **14**: 240082.

<https://doi.org/10.1098/rsob.240082>

Received: 2 April 2024

Accepted: 23 October 2024

### Subject Areas:

biochemistry, molecular biology

### Keywords:

protein quantification, transmembrane proteins, ELISA, Na,K-ATPase

### Authors for correspondence:

Shabnam Mohammadi

e-mail: [smohammadi@ice.mpg.de](mailto:smohammadi@ice.mpg.de)

Susanne Dobler

e-mail: [susanne.dobler@uni-hamburg.de](mailto:susanne.dobler@uni-hamburg.de)

<sup>†</sup>Joint first authors.

<sup>‡</sup>Joint senior authors.

Electronic supplementary material is available online at <https://doi.org/10.6084/m9.figshare.c.7547683>.

# Evaluating the efficacy of protein quantification methods on membrane proteins

Jana Löptien<sup>1,†</sup>, Sidney Vesting<sup>1,†</sup>, Susanne Dobler<sup>1,‡</sup> and Shabnam Mohammadi<sup>1,2,‡</sup>

<sup>1</sup>Molecular Evolutionary Biology Institute of Cell and Systems Biology of Animals, Universität Hamburg, Hamburg, Germany

<sup>2</sup>Max Planck Institute for Chemical Ecology, Jena, Germany

JL, 0009-0003-8180-9978; SD, 0000-0002-0635-7719; SM, 0000-0003-3450-6424

Protein quantification is an important tool for a wide range of biological applications. The most common methods include the Lowry, bicinchoninic acid (BCA) and Coomassie Bradford assays. Despite their wide applicability, the mechanisms of action imply that these methods may not be ideal for large transmembrane proteins due to the proteins' integration in the plasma membrane. Here, we investigate this problem by assessing the efficacy and applicability of these three common protein quantification methods on a candidate transmembrane protein: Na, K-ATPase (NKA). We compared these methods with an ELISA, which we newly developed and describe here for the quantification of NKA. The use of a relative standard curve allows this ELISA to be easily adapted to other proteins and across the animal kingdom. Our results revealed that the three conventional methods significantly overestimate the concentration of NKA compared with the ELISA. This is due to the samples containing a heterogeneous mix of proteins, including a significant amount of non-target proteins. Further, by applying the protein concentrations determined by the different methods to *in vitro* assays, we found that variation in the resulting data was consistently low when the assay reactions were prepared based on concentrations determined from the ELISA.

## 1. Introduction

Many biological applications rely on protein quantification. These include biochemical assays that assess the function of proteins [1,2], the assessment of protein abundances between tissues and species [3], and the assessment of knockdown experiments [4]. The most common all-encompassing methods of protein quantification include the Lowry, bicinchoninic acid (BCA) and Coomassie Bradford assays [5–7]. In general, these methods are sensitive, simple, inexpensive and easily reproducible [8]. Moreover, they are available as standardized commercial kits. In all three methods, total protein concentration is detected by a colour signal whose intensity correlates with the quantity of total protein present in the sample and which can be measured spectrophotometrically.

Yet, despite their popularity, all three methods have shortcomings. Both the Lowry and BCA assays rely on the reduction of copper ions by peptide bonds, and thus the more peptide bonds are accessible, the higher the determined protein concentration will be [5,6,9]. In addition, all three methods are sensitive to the presence of specific amino acids, resulting in stronger staining of proteins with higher frequency of these amino acids. An additional clear drawback is that they detect all proteins in a given sample and can thus

only provide an estimate for specific protein concentrations when samples contain unpurified or partially purified proteins. Moreover, all three methods exhibit some degree of detection variation towards different protein types and the popular Bradford assay is sensitive to substances that are routinely used to lyse cells and solubilize membrane proteins, such as detergents, which compete with the dye for binding sites [7,10].

Another challenge for these conventional methods is transmembrane proteins, which are largely embedded in the cell's hydrophobic lipid bilayer. The Bradford assay has already been shown to underestimate the protein concentration of membrane-containing fractions due to the significant portion of membrane proteins being embedded in the cell membrane and thus not accessible to the dye molecules [11]. Therefore, experimental work with such proteins has often relied on relative protein quantification by a combination of Bradford assays and western blots [12–16]. While these methods can be sufficient for estimating protein concentrations across samples, they lack the precision needed for producing robust measurements, especially when target protein concentrations vary across biological replicates. Moreover, western blots are labour-intensive, and are not ideal for explicit quantification.

Enzyme-linked immunosorbent assays (ELISAs) present a solution for quantifying large transmembrane proteins and overcome some of the limitations and drawbacks associated with the conventional methods as they target specific proteins in a sample. The interaction between antigen and antibody allows the quantification of small amounts of a specific target protein in a heterogeneous sample [17,18].

Three types of ELISAs have been developed: sandwich, direct and indirect. A sandwich ELISA is the most precise method because the target protein is bound between two primary antibodies (capture antibody and detection antibody), each detecting a different epitope of the target protein. However, this method requires a lot of tailoring for each protein type and is thus not easily applicable across a broad range of proteins. A direct ELISA uses a single primary antibody, which also serves as the detection antibody, allowing the direct detection of the target protein. An indirect ELISA relies on a secondary antibody to detect the primary antibody. A standard secondary antibody can be applied to different primary antibodies, and the primary antibody does not require any labelling. The indirect ELISA is thus the most easily applicable method. Although a variety of commercial ELISA kits are available for different proteins, they are expensive, specific for only a narrow range of protein sources (e.g. rats, mice, humans) and can be ineffective depending on the protein isolation methods.

To address the challenge of accurate transmembrane protein quantification, we compare the three conventional methods (Lowry, BCA and Bradford) and evaluate their performance in detecting and quantifying transmembrane proteins in comparison with an indirect ELISA, which we newly developed and validate here. We use Na, K-ATPase (NKA) as our model protein. This transmembrane protein has been studied extensively in our working group and we have established a high-throughput expression system to produce NKA from a wide range of taxa. The smallest functional unit of the NKA consists of a dimer of a large  $\alpha$ -subunit with 10 transmembrane helices and a glycosylated  $\beta$ -subunit of one transmembrane helix [19,20].

The ELISA developed for NKA in this paper makes use of a commercially available primary antibody, which binds universally across the animal kingdom. We additionally developed a method for producing relative standards by lyophilizing an aliquot of the protein being measured. These specifications allow our ELISA to be adapted to any protein type and source.

## 2. Material and methods

All key resources and reagents used in this study are listed in detail in electronic supplementary material, table S1.

### 2.1. Acquiring expression vectors

The majority of our protein samples were produced by expression in cell culture. This allowed us to sample from a broader range of taxa. We used six pFastBac Dual plasmids, which have two cloning sites for the simultaneous expression of two proteins, containing the NKA  $\alpha$ 1- and  $\beta$ 1-subunit genes from six different animal species. The species included the brown rat (*Rattus norvegicus*), common ostrich (*Struthio camelus*), gold tegu (*Tupinambis teguixin*), large milkweed bug (*Oncopeltus fasciatus*), Miranda's white-lipped frog (*Leptodactylus macrosternum*) and red-necked keelback snake (*Rhabdophis subminiatus*). We selected these species because we wanted to sample as broad a range of animals as possible. All vertebrate vectors were originally produced by Mohammadi *et al.* [1,16] and the large milkweed bug vector was produced by S. Dalla [21]. Each vector had the  $\alpha$ 1-subunit gene (ATP1A1 for vertebrates, ATP $\alpha$ 1C for the large milkweed bug) under the control of the P<sub>PH</sub> promoter and the  $\beta$ -subunit gene (ATP1B1 for vertebrates,  $\beta$ 1 for the large milkweed bug) under the p<sub>10</sub> promoter. Accession numbers for the sequences and the Addgene plasmid numbers associated with these plasmid constructs can be found in electronic supplementary material, table S2.

### 2.2. Bacmid production

The six recombinant plasmids were transposed into competent DH10Bac *Escherichia coli* cells and grown on plates containing gentamycin, tetracycline, kanamycin, isopropyl  $\beta$ -D-1-thiogalactopyranoside (IPTG), X-Gal. DH10Bac cells contain a bacmid and a helper plasmid. The transposed donor plasmid segment contains the inserted ATP1A1 and ATP1B1 genes, along with a gentamicin resistance gene, and recombines at the lacZ alpha peptide gene on the bacmid, disrupting its reading frame. The resulting colonies are white when grown on plates containing IPTG and X-Gal, whereas those with intact lacZ proteins (i.e. failed recombination) are blue. Following transposition, two white colonies were picked from each plate (per NKA construct) and incubated in liquid culture containing gentamycin, tetracycline and kanamycin to amplify the recombinant bacmids.

The amplified bacmid DNA was isolated from *E. coli* cells via alkaline lysis. Briefly, the *E. coli* cells were lysed with a strong alkaline solution consisting of 200 mM NaOH and 1% SDS. Cell debris, SDS and genomic DNA were removed by centrifugation, and the resulting bacmid DNA was pelleted and washed with 70% ethanol. The pellet was resuspended in purified water and the resulting bacmid DNA was analysed by PCR and agarose gel electrophoresis to verify that the transposition of the genes of interest to the bacmids was successful (electronic supplementary material, figure S1). The primers used for this analysis were pUC/M13 FWD 5'-CCCAGTCACGACGTTGAAAACG-3' and pUC/M13 RVS 5'-AGCGGATAACAATTCACACAGG-3'.

### 2.3. Generation of recombinant baculoviruses and expression of NKA proteins in Sf9 cells

Sf9 cells (immortalized ovary cells from the moth *Spodoptera frugiperda*) were used as the host for recombinant baculovirus production and protein expression. Sf9 cells are advantageous for NKA expression because they express very little of the protein endogenously [22,23].

We followed the modified one-step protocol described by Scholz & Suppmann [24]. For baculovirus production,  $8 \times 10^6$  Sf9 cells in 10 ml Insect-Xpress medium with  $30 \mu\text{g ml}^{-1}$  gentamycin were transfected with 10  $\mu\text{g}$  purified bacmid DNA using PEI MAX. We repeated this procedure three times to produce three biological replicates (A, B, C) per NKA construct. After 5 days of incubation at 27°C and 110 rpm, the Sf9 cells were pelleted by centrifugation at  $500 \times g$  for 5 min and the P0 viruses in the supernatant were harvested. Freshly seeded Sf9 cells ( $50 \times 10^6$  cells in 50 ml media) were subsequently infected with the P0 viruses (500  $\mu\text{l}$  virus per biological replicate). Following 3 days of incubation at 27°C and 110 rpm, the Sf9 cells were pelleted by centrifugation at  $1650 \times g$  for 10 min and stored at -80°C until membrane isolation. Additionally, untransfected Sf9 cells (i.e. without NKA expression) were also cultured ( $25 \times 10^6$  cells in 50 ml media) and pelleted for use as a negative control.

### 2.4. Membrane isolation from Sf9 cells

The frozen Sf9 cell pellets were resuspended in 15 ml of homogenization buffer (0.25 M sucrose, 2 mM EDTA, 25 mM HEPES; adjusted to pH 7.0 with Tris HCl) on ice. The cell suspensions were then sonicated at 60 W (Sonopuls 2070) for three 45 s intervals on ice to lyse the cells and disrupt the cell membranes. Next, the cell suspensions were centrifuged for 30 min at  $10\,000 \times g$  and 4°C (Centrifuge 5840 R) to pellet cell debris. The supernatant was collected and further centrifuged for 60 min at  $146\,000 \times g$  and 4°C (Ultra-Centrifuge L-80) to pellet the cell membranes. The supernatant was removed, and the pelleted membranes were washed twice and resuspended in cooled HPLC grade water (1 ml per biological replicate), then stored at -20°C.

### 2.5. Preparation of tissue samples

Brain and kidney tissue was dissected from three freshly frozen black rats purchased commercially from frostmaus.de. Nervous tissue (brains, prothoracic and central ganglia) was also dissected out of 14 freshly frozen large milkweed bugs and pooled into one sample. The bugs were acquired from a colony reared at University of Hamburg [25]. All tissue samples were homogenized on ice with a glass grinder in 500  $\mu\text{l}$  HPLC grade water. Nervous tissue samples were lyophilized overnight (12–24 h) at 0.1 mbar and -50°C in a freeze dryer. After lyophilization, the freeze-dried samples were resuspended in 500  $\mu\text{l}$  (large milkweed bug) or 1 ml (black rat) cooled HPLC grade water. The resuspended samples were then sonicated in an ice bath for 10 min (Omni Sonic Ruptor 400, Pulser 90, Power 90%) and centrifuged for 10 min at  $5000 \times g$  and 4°C (Centrifuge 5840 R) to precipitate debris. The resulting supernatant was stored at -20°C. Membranes from kidney samples were isolated as described above for Sf9 cells. Nervous tissue is known to have very high levels of NKA expression compared with other tissues [26–29]. Therefore, we deemed it unnecessary to concentrate the proteins by isolating membranes for this tissue.

### 2.6. Positive control

A lyophilized sample of commercially available, purified NKA from porcine cerebral cortex (0.3 units  $\text{mg}^{-1}$  protein; electronic supplementary material, table S1) was resuspended to a stock concentration of 10  $\text{mg ml}^{-1}$  in HPLC grade water (i.e. 10 mg dry powder suspended in 1 ml water).

### 2.7. Testing the effect of lyophilization on antibody detection

We wanted to prepare relative standards for our ELISA by using the dry weight of lyophilized protein samples containing NKA from different species. We therefore first tested whether lyophilizing NKA would cause a reduction in their detection by antibodies. For this comparison, we used a 300  $\mu\text{l}$  aliquot of membrane isolated samples derived from Sf9 cell expression (table 1), which consisted of 100  $\mu\text{l}$  of each replicate (A–C) pooled together. For common ostrich and Miranda's white-lipped frog, 162.5  $\mu\text{l}$  of replicates A and B were pooled because the C replicates were contaminated during the preparation process. The samples were dried overnight (12–24 h) at 0.1 mbar and -50°C in a freeze dryer. Afterwards, the samples were centrifuged shortly and their weights calculated by subtracting the weight of the empty tubes. The freeze-dried samples were then resuspended in 200–300  $\mu\text{l}$  cooled HPLC grade water. An aliquot was taken from each sample for the downstream production of relative standards.

**Table 1.** List of protein samples used in this study. Protein samples derived from tissue are highlighted in grey, all others were expressed in Sf9 cells.

order	species	NKA source	used for
Mammalia	<i>Rattus norvegicus</i> (brown rat)	expressed in Sf9 cells	(1) testing effects of lyophilization (2) relative NKA standard production (3) comparing protein quantification methods (4) comparing applicability of quantification methods
Mammalia	<i>Rattus rattus</i> (black rat)	brain tissue preparation	(3) comparing protein quantification methods (4) comparing applicability of quantification methods
Mammalia	<i>Rattus rattus</i> (black rat)	kidney tissue preparation	(3) comparing protein quantification methods (4) comparing applicability of quantification methods
Mammalia	<i>Sus domesticus</i> (porcine)	commercially available, lyophilized cerebral cortex NKA isolate	(2) NKA standard production (3) comparing protein quantification methods —positive control
Aves	<i>Struthio camelus</i> (common ostrich)	expressed in Sf9 cells	(1) testing effects of lyophilization (2) relative NKA standard production (3) comparing protein quantification methods (4) comparing applicability of quantification methods
Squamata	<i>Tupinambis teguixin</i> (gold tegu)	expressed in Sf9 cells	(1) testing effects of lyophilization (2) relative NKA standard production (3) comparing protein quantification methods (4) comparing applicability of quantification methods
Squamata	<i>Rhabdophis subminiatus</i> (red-necked keelback snake)	expressed in Sf9 cells	(1) testing effects of lyophilization (2) relative NKA standard production (3) comparing protein quantification methods (4) comparing applicability of quantification methods
Amphibia	<i>Leptodactylus macrosternum</i> (Miranda's white-lipped frog)	expressed in Sf9 cells	(1) testing effects of lyophilization (2) relative NKA standard production (3) comparing protein quantification methods
Insecta	<i>Oncopeltus fasciatus</i> (large milkweed bug)	expressed in Sf9 cells	(1) testing effects of lyophilization (2) relative NKA standard production (3) comparing protein quantification methods (4) comparing applicability of quantification methods
Insecta	<i>Oncopeltus fasciatus</i> (large milkweed bug)	brain and ganglia tissue preparation	(3) comparing protein quantification methods
Insecta	untransfected Sf9 cells (ovary cells from <i>Spodoptera frugiperda</i> )	Sf9 cells (contain very little to no endogenous NKAs)	(1) testing effects of lyophilization (3) comparing protein quantification methods —negative control

For the western blot analysis, 2.5 µl of non-lyophilized and resuspended lyophilized samples were solubilized in 8 µl 4× Laemmli buffer (62.5 mM Tris HCl pH 6.8; 2% SDS; 10% glycerol; 5% 2-mercaptoethanol; 0.001% Bromophenol Blue) and 21.5 µl Millipore water. The solubilized samples were then separated on an SDS gel containing 10% acrylamide. Subsequently, the separated proteins were blotted from the gel onto nitrocellulose membrane. To block unsaturated binding sites on the membranes after blotting, they were incubated at room temperature in 1× BlueBlock PF on a plate tipper at medium tipping speed for 1 h. After blocking, the membranes were transferred into a 50 ml Falcon tube and incubated with 2 ml of the primary antibody (electronic supplementary material, table S1) at a concentration of 0.88 µg ml<sup>-1</sup> in 1× BlueBlock PF overnight at 4°C on a tube rotator. Next, the membranes were washed three times with 1× BlueBlock PF. The membranes were then incubated with 2 ml of the secondary antibody (electronic supplementary material, table S1) at a concentration of 8 µg ml<sup>-1</sup> in 1× BlueBlock PF for 1 h at room temperature on the tube rotator. Next, the membranes were washed three times with 1× BlueBlock PF and two additional times with 0.05 M Tris HCl for 5 min each. The antibody complexes were stained by moving the membranes into a glass petri dish and adding the detection enzyme substrate (0.035% H<sub>2</sub>O<sub>2</sub>, and 0.01% 4-chloro-1-naphthol in 0.05 M, pH 7.5 Tris HCl). Following a 10 min incubation, the staining reaction was stopped by washing the membrane with deionized water. The resultant membranes were scanned (Canon 9000F Mark II). These samples were also compared on our ELISA (described



below) and the results from both the western blot and ELISA were statistically compared (described below). See electronic supplementary material, table S3, for raw data.

In addition to the western blot analysis, we ran one replicate (replicate A) from each recombinant protein produced for the relative standards on an SDS-PAGE gel followed by Coomassie Blue staining to determine how much of the protein samples consists of the target-protein (i.e. the NKA  $\alpha$ -subunit). We calculated the intensity density of the protein content of the whole lane and the target  $\alpha$ -subunit band using ImageJ v1.53. Comparing the two values revealed that the  $\alpha$ -subunit makes up on average 1.8% of the total protein content of the membrane isolates (electronic supplementary material, figure S2). We used this value to adjust our ELISA relative standard curves, described further down. The presence of lipids in our samples remains unquantified. However, the consistency of our protein expression system mitigates potential variations arising from unmeasured lipid quantities. This consistency is enforced by using the same number of cells across infections and by using the same cell lines throughout the protocol. Such consistency would be challenging to achieve when using tissue-isolated samples or different cell types. As a result, we did not generate standard curves from tissue-derived samples.

## 2.8. Protein assays

All the protein samples we produced were quantified by Lowry, BCA, Bradford and ELISA. The commercial porcine sample was used as a positive control, and the protein sample derived from untransfected Sf9 cells was used as a negative control for all four methods. All four assays were run on aliquots that were not previously freeze-thawed.

## 2.9. Lowry protein assay

We used Thermo Fisher Scientific's Modified Lowry protein assay kit (electronic supplementary material, table S1). First, a standard curve was prepared with bovine serum albumin (BSA) (1500, 1000, 750, 500, 250, 125, 25, 5, 1 and 0  $\mu\text{g ml}^{-1}$ ) in Millipore water. The protein samples were diluted 1:10 in Millipore water, except for porcine and large milkweed bug tissue samples, which were not diluted because low protein content was expected in these samples. Forty microlitres of the standards and protein samples were pipetted in duplicate (two technical replicates) into 96-well polystyrene flat-well plate wells. Two hundred microlitres of Lowry reagent was added to each well, mixed on a microplate shaker for 30 s, and then incubated at room temperature for 10 min. Following incubation, 20  $\mu\text{l}$  of freshly prepared 1 $\times$  Folin-Ciocalteu reagent was added to each well and mixed on the microplate shaker for 30 s. Following a 30 min room temperature incubation, the absorbance of standards and protein samples was measured at 655 nm using a microplate absorbance reader (Bio-Rad Model 680). See electronic supplementary material, table S4, for raw Lowry assay data.

## 2.10. Bicinchoninic acid protein assay

We used Thermo Fisher Scientific's Bicinchoninic acid protein assay kit (electronic supplementary material, table S1). First, a standard curve was prepared with BSA (1500, 1000, 750, 500, 250, 125, 25, 5, 1 and 0  $\mu\text{g ml}^{-1}$ ) in Millipore water. The protein samples were diluted 1:10 in Millipore water, except for porcine and large milkweed bug tissue samples, which were not diluted. Twenty-five microlitres of the standards and protein samples were pipetted in duplicate (two technical replicates) into 96-well polystyrene flat-well plate wells. Two hundred microlitres of freshly prepared, clear, green BCA working reagent was added to each well, and mixed on a microplate shaker for 30 s. Following a 30 min incubation at 37°C and subsequent cooling of the plate to room temperature, the absorbance of standards and protein samples was measured at 550 nm using a microplate absorbance reader (Bio-Rad Model 680). See electronic supplementary material, table S5, for raw BCA assay data.

## 2.11. Coomassie Bradford protein assay

For the Bradford assay, we prepared a standard curve with BSA (10, 8, 6, 4, 2 and 0  $\mu\text{g ml}^{-1}$ ) in Millipore water. The protein samples derived from Sf9 cells and rat brain tissue were diluted 1:2000 in Millipore water, whereas porcine and large milkweed bug tissue samples were diluted 1:200 (see §2 above). Both the standards and protein samples were then diluted 1:2 with Coomassie Bradford reagent and pipetted into polystyrene cuvettes in duplicate (two technical replicates). After incubating at room temperature for 10 min, the absorbance of standards and protein samples was measured at 595 nm using a cuvette spectrophotometer (Ultrospec 2100 pro). See electronic supplementary material, table S6, for raw Bradford assay data.

## 2.12. Relative NKA standard preparation for the ELISA

For each animal species to be assayed, a relative NKA standard was prepared from the lyophilized membrane isolates derived from Sf9 cells (figure 1). The concentration of each standard was calculated based on their lyophilized weights (described above). These concentrations were used to create relative NKA standard stock aliquots of 1 mg  $\text{ml}^{-1}$  in ELISA coating buffer (0.1 M  $\text{NaHCO}_3$  in PBS, adjusted to pH 9.5 with KOH; electronic supplementary material, table S7) for each animal species.

## 2.13. Indirect ELISA to quantify NKA proteins

Prior to running an ELISA, the protein samples were diluted 1:2000 in the coating buffer (electronic supplementary material, table S7). Replicates A–C of common ostrich and large milkweed bug were diluted 1:6000 and 1:4000, respectively, because

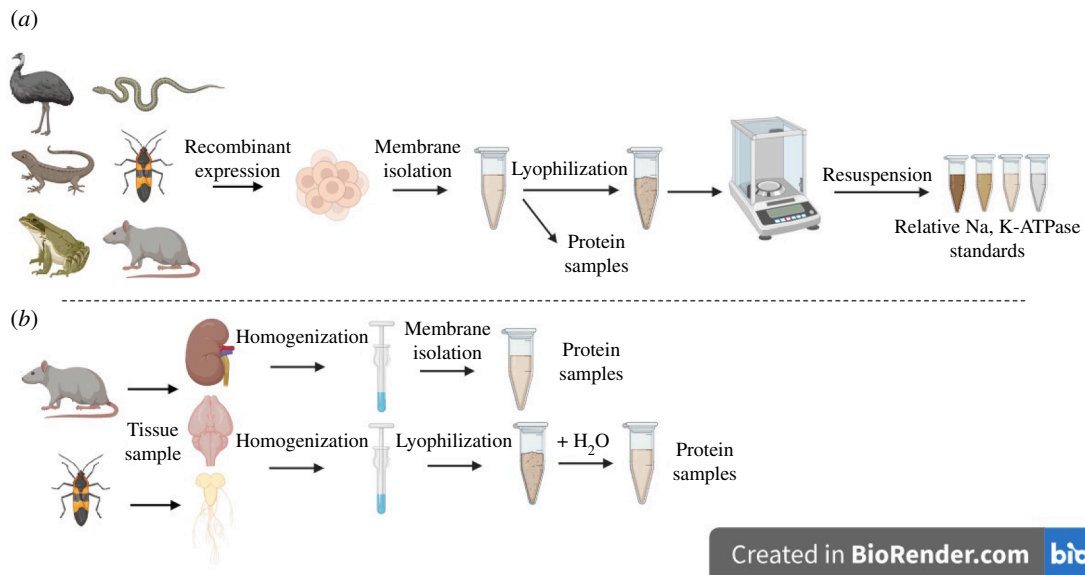


**Figure 1.** Schematic diagram illustrating the isolation of proteins (a) from recombinant expression in Sf9 cells and (b) from tissues. Nervous tissue samples were isolated by homogenization, followed by centrifugation to pellet waste, and lyophilization, whereas all other samples were membrane isolated. Relative Na, K-ATPase (NKA) standards were subsequently prepared from a subset of membrane isolates from recombinantly expressed Sf9 cells. All resulting protein samples were used in all four quantification assays, while the relative NKA standards were produced specifically for the ELISA. Figure created with BioRender.com.

higher NKA concentrations were expected in these samples based on the western blots. The  $1 \text{ mg ml}^{-1}$  relative NKA standard stocks were sonicated in an ice bath for two 2.5-min intervals (Omni Sonic Ruptor 400, Pulser 90, Power 90%). Using dry weight and adjusting to account for the 1.8%  $\alpha$ -subunit content (electronic supplementary material, figure S2), the standards were diluted in coating buffer to the following concentrations: 0.01125, 0.016875, 0.0225, 0.03375, 0.045, 0.0675, 0.09, 0.135, 0.18, 0.27, 0.36, 0.54 and  $1.08 \text{ } \mu\text{g ml}^{-1}$ . This concentration range corresponds to the following dry weight: 0.625, 0.9375, 1.25, 1.875, 2.5, 3.75, 5, 7.5, 10, 15, 20, 30 and  $60 \text{ } \mu\text{g ml}^{-1}$ . The same dry weights were used to produce the standards for the commercial porcine NKA but were adjusted for a 14.4% target-protein content, as indicated by the certificate of analysis (electronic supplementary material, table S1). Thus, the commercial porcine NKA standard range was as follows: 0.09, 0.135, 0.18, 0.27, 0.36, 0.54, 0.72, 1.08, 1.44, 2.16, 2.88, 4.32 and  $8.64 \text{ } \mu\text{g ml}^{-1}$ . All ELISAs were run on aliquots that were not previously freeze-thawed.

First,  $100 \text{ } \mu\text{l}$  of protein samples and relative NKA standards were added to 96-well polystyrene flat-well plates in duplicate (two technical replicates). Additionally,  $100 \text{ } \mu\text{l}$  of a negative control using only coating buffer without any protein was added to the plates. This negative control is equal to the  $0 \text{ } \mu\text{g ml}^{-1}$  standard. After adding samples and standards to the wells, the plates were sealed with Parafilm and incubated overnight at  $4^\circ\text{C}$  (12–18 h).

The next day, unbound leftovers were discarded and plates dried by tapping them several times face-down on a paper towel. Each well was washed by adding  $400 \text{ } \mu\text{l}$  of washing buffer (0.05% Tween 20 in PBS; electronic supplementary material, table S7), letting it sit for 10 s, then discarding fluids as described above. This washing procedure was repeated to a total of five times. Next, unsaturated surface-binding sites were blocked by adding  $200 \text{ } \mu\text{l}$  of blocking buffer (1% BSA, 0.02% Tween 20 in PBS; electronic supplementary material, table S7) to each well, sealing the plates with Parafilm, and incubating at room temperature for 2 h. Following blocking, the wells were washed as described above.

We used the universal monoclonal primary antibody  $\alpha 5$  to detect the NKA  $\alpha$ -subunit ( $\alpha 5$ -antibody; electronic supplementary material, table S1). The antigen species for this antibody is chicken and the host species is mouse. The  $\alpha 5$ -antibody binds a cytosolic epitope on the  $\alpha$ -subunit of all NKA isoforms across the animal kingdom. Fifty microlitres of primary antibody solution containing  $2 \text{ } \mu\text{g ml}^{-1}$   $\alpha 5$ -antibody in blocking buffer was added to each well, and left to incubate, sealed with Parafilm, for 1 h at room temperature (overnight (12–18 h) at  $4^\circ\text{C}$  is also possible).

To remove unbound primary antibodies, the wells were washed as described above. Next, we used a goat-anti-mouse polyclonal secondary antibody conjugated with horseradish peroxidase (HRP-antibody; electronic supplementary material, table S1) to detect the primary antibody. The host species for the secondary antibody is goat. Fifty microlitres of secondary antibody solution containing  $5 \text{ } \mu\text{g ml}^{-1}$  HRP-antibody in blocking buffer was added to each well, and left to incubate, sealed with Parafilm, for 1 h at room temperature.

Following the secondary antibody incubation, each well was washed seven times as described above to maximally reduce background noise caused by unbound HRP-antibody. The colorimetric reaction of HRP was triggered by adding  $100 \text{ } \mu\text{l}$  3,3',5,5'-tetramethylbenzidine (TMB) to each well, and allowing colour development at room temperature for 10 min. The colorimetric reaction was stopped by adding  $100 \text{ } \mu\text{l}$  stopping solution ( $0.5 \text{ M H}_2\text{SO}_4$ ) to each well. Finally, the absorbance of standards and protein samples was measured at  $490 \text{ nm}$  using a microplate absorbance reader (Bio-Rad iMark). See figure 2 for a schematic diagram of the ELISA methods and electronic supplementary material, table S7, for buffer recipes.

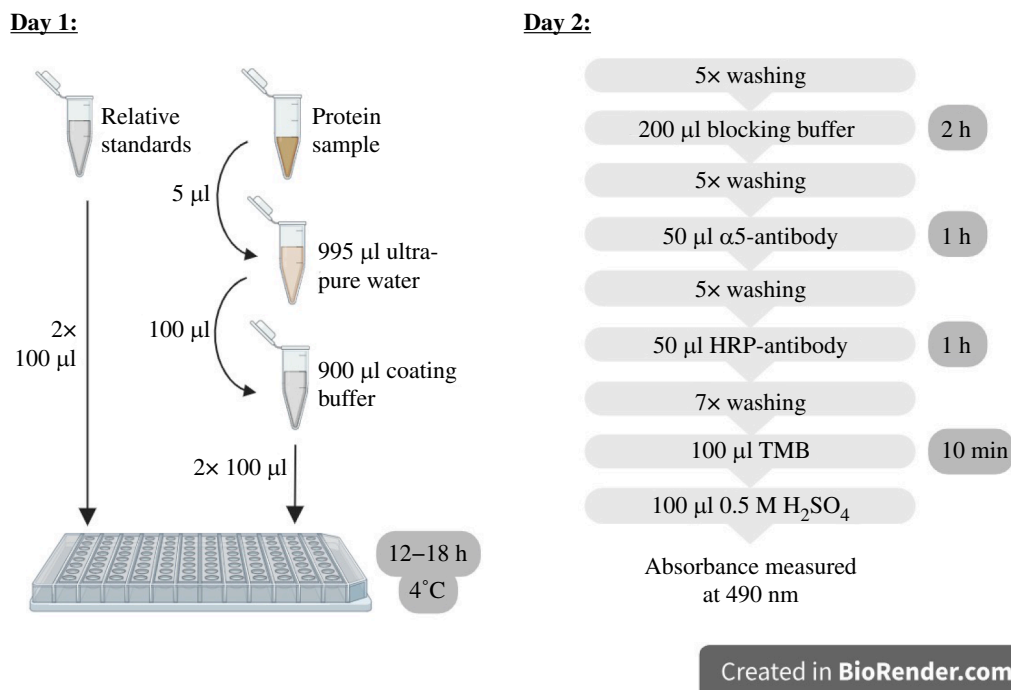


**Figure 2.** Schematic diagram illustrating the two-day ELISA procedure. Figure created with [BioRender.com](https://www.biorender.com).

## 2.14. Negative controls

Several negative controls were included to validate the functionality of this ELISA. First, the primary antibody ( $\alpha 5$ -antibody) was omitted to confirm that there is no non-specific binding of the secondary HRP-antibody. Next, the HRP-antibody was omitted to confirm that TMB and the stopping solution do not stain non-specifically (i.e. without HRP). For these negative controls, a random sample from our Sf9 expressed proteins was used (gold tegu replicate A). Then, both protein and antibodies were omitted to confirm that there is no background noise caused by the buffers. Finally, membrane isolate of untransfected Sf9 cells was run in the ELISA with the gold tegu standards to confirm that the antibodies are not binding non-specifically to other membrane proteins. See electronic supplementary material, table S8, for raw negative control data.

## 2.15. Calculation of protein concentrations

For all protein quantification methods, the average absorbance of the two blank standard replicates ( $0 \mu\text{g ml}^{-1}$ ) was subtracted from each absorbance measurement. Then, the average values of the two technical replicates were calculated. The average absorbance values of each standard were used for a linear trendline-fitting. For the ELISA, the standards often reached saturation at higher concentration ranges. We therefore used a nonlinear sigmoidal trendline-fitting according to Fedosov *et al.* [30]. See electronic supplementary material, table S9, for raw ELISA data and electronic supplementary material for the corresponding R code.

## 2.16. Testing the robustness of protein quantification methods with *in vitro* NKA activity assays

To examine the robustness of the determined protein or NKA concentrations, the variation across biological replicates of *in vitro* NKA activity assays were compared. Only animal species with three or more biological replicates were tested in the NKA activity assays. Thus, Miranda's white-lipped frog and large milkweed bug tissue were excluded from the assays. Replicate C of Miranda's white-lipped frog encountered infection problems during transfection whereas the number of large milkweed bugs we dissected was only sufficient to produce one biological replicate for the tissue. For each assay,  $100 \mu\text{g}$  of protein was used and this was calculated based on concentrations determined by the four different protein quantification methods. Because we ran these assays prior to the SDS-PAGE and prior to correcting the standard concentrations based on the  $\alpha$ -subunit content, the protein input for the ELISA represents concentrations calculated from the weighted range of  $0 \text{ mg ml}^{-1}$  to  $60 \text{ mg ml}^{-1}$ . Further, the original ELISA protein input was based on previous linear fitted curves, which have now been improved with sigmoidal fitted curves. This slightly shifted the protein content for some samples, however, all remained within close range of  $100 \mu\text{g}$ .

The  $100 \mu\text{g}$  of protein was pipetted in duplicate (two technical replicates) into two wells on a 96-well polystyrene flat-well plate. The first well contained stabilizing buffer to measure total ATPase activity and the second well contained inhibiting buffer (lacking KCl and including  $10^{-2} \text{ M}$  ouabain) to block NKAs and measure background ATPase activity. See assay buffer formulas in Petschenka *et al.* [31]. The proteins were incubated at  $37^\circ\text{C}$  and 200 rpm for 10 min on a microplate shaker.

Next, ATP ( $10 \text{ mM}$  Tris-ATP, pH 6.5) was added to each well and the proteins were incubated again at  $37^\circ\text{C}$  and 200 rpm for 20 min. The activity of NKAs was determined by quantification of inorganic phosphate ( $\text{P}_i$ ) released from enzymatically hydrolysed ATP. Reaction  $\text{P}_i$  levels were measured according to the procedure described by Petschenka *et al.* [31]. The reactions

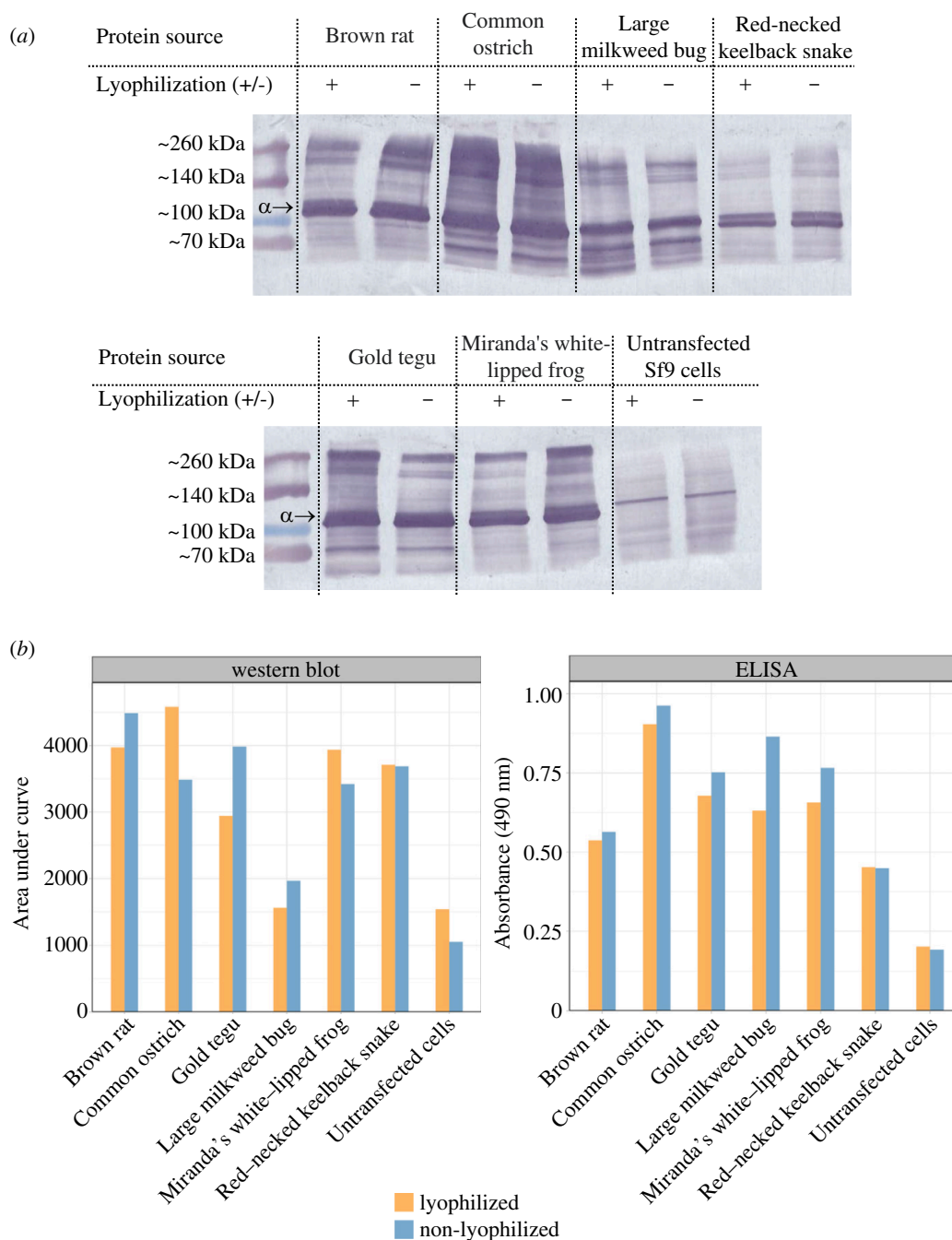


**Figure 3.** (a) Western blot membrane scans show lyophilized and non-lyophilized Sf9 cell membrane isolates run on two gels. The 110 kDa line corresponds to the NKA's  $\alpha$ -subunit, which is marked by an arrow. Because the  $\alpha 5$  primary antibody is specific only to the NKA  $\alpha$ -subunit, additional bands and smearing are most likely caused by higher order complexes and high protein load. The + and - indicate which bands are lyophilized (+) and which are not (-). (b) Comparison of detection intensity between lyophilized and non-lyophilized Sf9 membrane isolates in the western blot and ELISA analyses. Densities of the western blot's NKA  $\alpha$ -subunit bands were determined by the areas under the curves in ImageJ (electronic supplementary material, figure S4, table S3).

were stopped with 10% SDS and then stained with a solution consisting of Taussky-Shorr colour reagent [32], which turned the reactions blue in proportion to their  $P_i$  concentration. After 10 min of staining, the absorbance of each well was measured at 655 nm using a microplate absorbance reader (Bio-Rad Model 680). Average absorbance values of the two technical replicates were used for subsequent calculations.

The averages of two technical replicates were translated to mM  $P_i$  based on a standard curve of  $KH_2PO_4$  (0–1.2 mM  $P_i$ ) that was run on the same plate. Background ATPase  $P_i$  concentrations were subtracted to obtain NKA ATPase  $P_i$  concentrations [31]. The  $P_i$  concentrations released from 100  $\mu$ g of protein were then converted to nmol  $P_i \div$  (mg protein  $\times$  min).

## 2.17. Statistical analyses

To test whether lyophilization alters NKA detection by antibodies, we compared the distribution of ELISA absorbance values between lyophilized and non-lyophilized samples with a Wilcoxon signed-rank test for paired samples. In addition, we compared the densities of the western blot's NKA  $\alpha$ -subunit bands (approx. 110 kDa) between the two treatments using ImageJ v. 1.53 [33] to draw plots from the signal strength and size of the western blot bands. From the resulting plots, the areas



under the curves were calculated. We then compared the distribution of the areas under the curves between lyophilized and non-lyophilized samples with a Wilcoxon signed-rank test for paired samples. For both analyses, the values for all samples were pooled together based on the treatment.

We used a Friedman rank sum test for paired samples to compare the NKA detection capabilities of the four different quantification methods. We first compared the concentration values between Sf9 and tissue-derived samples and found a significant difference (Wilcoxon paired test;  $p < 0.0001$ ). We thus continued by analysing Sf9 and tissue-derived samples separately. The positive control (commercial porcine sample), the negative control (untransfected Sf9 cells) and replicate C of Miranda's white-lipped frog (which was infected by bacteria in cell culture) were excluded from this analysis. For the remaining, determined protein concentrations of different samples were pooled for each quantification method, respectively. A two-sided Dunn's post hoc test (R package 'rstatix' [34]) was used to identify the quantification methods that significantly differ from one another in the distribution of their determined protein concentrations. Since multiple pairwise comparisons were performed simultaneously in this test, the Bonferroni adjustment method was used for controlling the family-wise error rate.

All statistical analyses were performed using R v. 4.1.1 software (R Core Team) and a significance level of 0.05 was applied. See electronic supplementary material, dataset S1, for data table used for statistical comparisons.

## 3. Results

### 3.1. Lyophilization does not affect NKA detection by antibodies

We found no significant difference between lyophilized and non-lyophilized samples (Wilcoxon signed-rank paired test;  $p = 0.81$ ;  $W = 16$ ;  $n = 7$ ; figure 3b). The ELISA corroborated the same result (Wilcoxon signed-rank paired test;  $p = 0.08$ ;  $W = 25$ ;  $n = 7$ ; figure 3b); showing no significant difference in the distribution of the absorbance values between the two treatments. These results confirm that lyophilization of Sf9 cell membrane isolates does not significantly diminish the detectability of the NKA proteins by the antibodies used in the ELISA.

### 3.2. Relative NKA standard curves vary between different animal species

Because the  $\alpha 5$  antibody can have different binding affinities to NKA from different animals, we produced a standard curve for each species. These standards were prepared from NKA expressed in Sf9 cells for consistency and reproducibility. In addition, we prepared standards from commercial porcine NKA. We found that most standard curves reached saturation well before the higher concentration range ( $0 \mu\text{g ml}^{-1}$  to  $1.08 \mu\text{g ml}^{-1}$ ; figure 4). The red-necked keelback snake standard was an exception to this pattern, for which the curve followed a more linear pattern. This could be due to lower binding affinity of the  $\alpha 5$  antibody to snake NKA, which can be seen by comparing the SDS-PAGE gel (electronic supplementary material, figure S2) to the western blot (electronic supplementary material, figure S3). The standards prepared from commercial porcine NKA exhibited a similar linear behaviour. Assuming the commercial porcine sample indeed contains predominantly NKA in membrane fragments, the plate wells are likely not being crowded by non-target proteins to the same extent as the wells containing recombinant proteins produced by us. Because of the high variation between these samples, having standards tailored to each animal group ensures that the concentrations of samples are not over- or underestimated in the ELISA. However, we believe that using the commercial porcine NKA as a general standard would also be appropriate, if the percentage of protein content is accounted for and the standard range is extended to cover higher absorption ranges.

### 3.3. NKA detection in ELISA assays is minimal to absent in negative controls

To assess the specificity of the antibodies used in the ELISA, several negative controls, which excluded different components of the ELISA, were tested. We set the detection threshold to 0.034, which is the average absorbance value of the reagents used in the ELISA (containing neither protein nor antibody). We found that the absorbance of the negative control containing no protein (i.e. membrane isolate) remained within this detection threshold (figure 5; electronic supplementary material, table S8). The negative control containing no HRP-conjugated secondary antibody fell slightly above this threshold. The negative control containing no primary  $\alpha 5$ -antibody minimally exceeded the detection threshold, which indicates that there is slight background noise caused by the HRP-conjugated secondary antibody. This is likely caused by unbound secondary antibody that remains in the well after repeated washing. In addition to these negative controls, we tested the NKA-specificity of the primary  $\alpha 5$ -antibody using membrane isolates of untransfected Sf9 cells, which express very little NKA endogenously [22,23]. There was some detection of NKAs in these membranes. This is expected because these cells express a small level of these proteins endogenously. In addition, untransfected cells have higher cell proliferation and thus membranes isolated from these samples will have a higher density of membranes than those isolated from transfected cells. Nevertheless, the detection of NKAs in samples derived from transfected Sf9 cells exceeded untransfected cells by more than twofold (figure 5). Together, these results confirm that the specificity of the ELISA for NKA is suitable.

### 3.4. Conventional protein quantification methods cannot sufficiently quantify NKA

Our comparisons between protein quantification methods revealed several notable patterns (figure 6a). In general, there was interspecies variation in protein concentrations among samples quantified by ELISA, which ranged between  $0.01$  to  $3.3 \text{ mg ml}^{-1}$ .

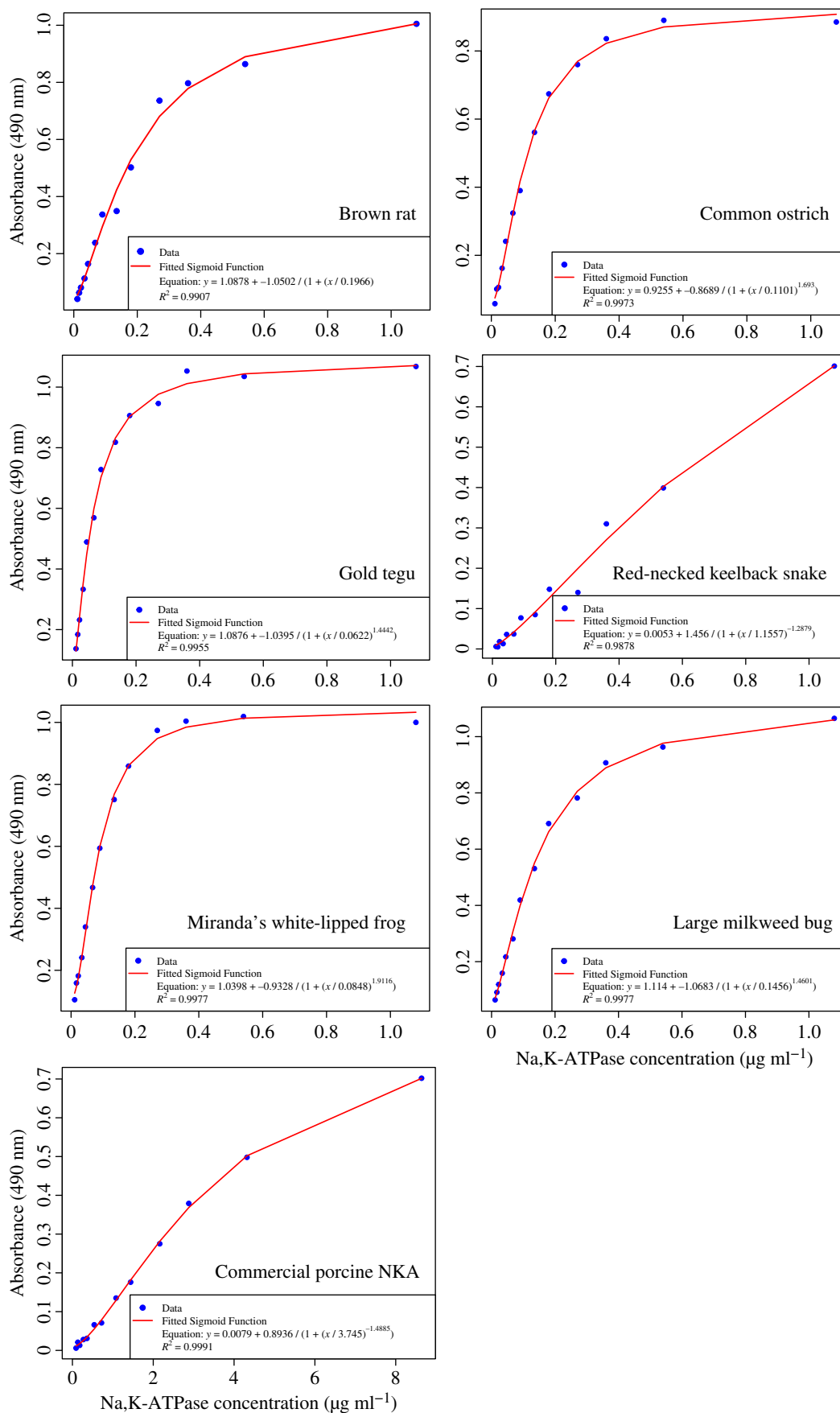


**Figure 4.** Comparison of standard curves generated from Sf9 cell membrane isolates containing recombinantly expressed Na, K-ATPase (NKA) from different animal species. Additionally, a standard curve prepared from commercial porcine NKA is included. Curves were fitted according to a sigmoidal fitting as described by equation 1A in Fedosov *et al.* [30].

This variation was more pronounced across the samples quantified by conventional methods, which ranged between 0.55 and 18.79 mg ml<sup>-1</sup> (electronic supplementary material, dataset S1).

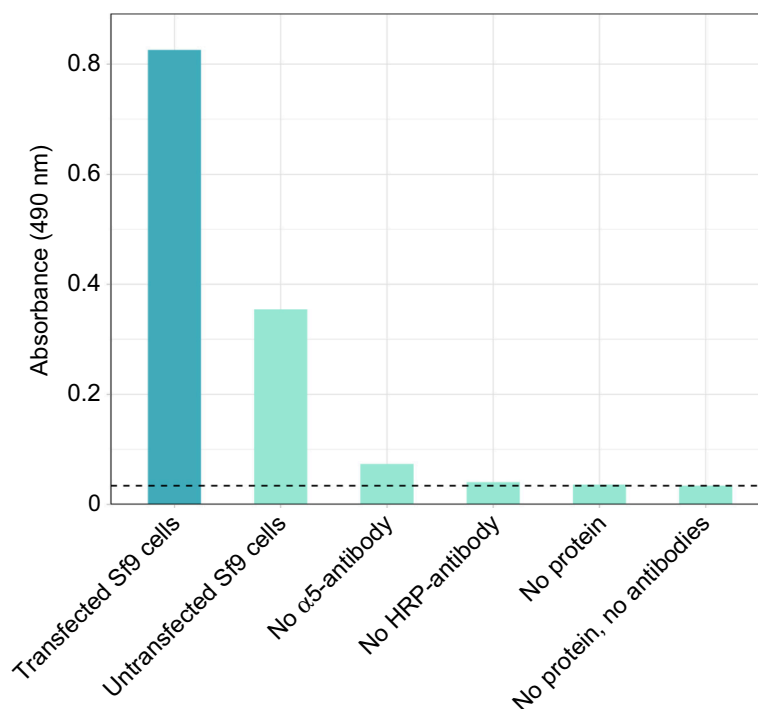


**Figure 5.** Comparison of ELISA absorbance values between a protein sample derived from transfected Sf9 cells (positive control; blue) and various negative controls (light turquoise). The positive control consisted of a gold tegu (replicate A) sample. This standard was subsequently used in the negative controls that contained protein (i.e. no  $\alpha 5$ -antibody and no HRP-antibody). The dashed line shows the detection threshold of ‘no protein, no antibodies’. Each bar represents the average of two technical replicates from one biological replicate.

Importantly, the three conventional methods detected more than  $7 \text{ mg ml}^{-1}$  in the negative control consisting of membrane isolates from untransfected Sf9 cells, whereas the ELISA detected less than  $1 \text{ mg ml}^{-1}$  (figure 6b). Since untransfected cells have higher viability, the rather high protein concentrations reflect the higher overall protein content resulting from higher cell density. The positive control consisting of purified porcine NKA, on the other hand, was quantified rather well by all three conventional quantification methods as below  $1.5 \text{ mg ml}^{-1}$ , with the Bradford coming closest to its actual concentration ( $10 \text{ mg ml}^{-1}$  based on lyophilized weight;  $1.44 \text{ mg ml}^{-1}$  based on 14.4% protein content; figure 6b; electronic supplementary material, dataset S1). By contrast, the ELISA determined a concentration of  $5.31 \text{ mg ml}^{-1}$ , which in this case is higher than the conventional methods. The closer match of the conventional methods could be due to the commercial porcine NKA content having been analysed by Biuret according to the certificate of analysis (electronic supplementary material, table S1). Taken together, these results suggest that the three conventional protein quantification methods significantly underestimate the concentration of NKA in a given sample, and likely other large transmembrane proteins.

To assess the NKA detection capabilities of the four different protein quantification methods, we pooled the determined concentrations of each method and statistically compared the resulting concentration distributions (figure 7a,b). We found that the protein concentration distributions for recombinantly expressed proteins were significantly different between the four methods (Friedman rank sum paired test;  $p < 0.001$ ;  $\chi^2 = 36.53$ ; d.f. = 3;  $n = 15$ ; figure 7a), with the ELISA having determined significantly lower protein concentrations compared with all three conventional methods (Dunn’s post hoc test; electronic supplementary material, table S10). By contrast, the three conventional methods did not significantly differ in their determined protein concentrations. We also found a significant difference in protein concentration distributions for tissue-isolated samples ( $p = 0.006$ ;  $\chi^2 = 12.6$ ; d.f. = 3;  $n = 9$ ; figure 7b). A post hoc Dunn’s test showed significantly lower protein concentrations determined by the ELISA compared with the other three methods (electronic supplementary material, table S10).

### 3.5. Quantification with ELISA consistently produces robust downstream ATPase assay data

To test whether the differences in protein quantification accuracy we uncovered affect downstream *in vitro* functional assays, ATPase activity assays were run based on protein concentrations determined by the four quantification methods. We tested whether the resulting variation in NKA ATPase activities (specified by standard deviation of NKA activity) significantly differs between the four quantification methods.

We did not detect a significant effect of protein quantification method on the mean standard deviation of NKA activities (ANOVA;  $p = 0.186$ ;  $F = 1.882$ ;  $n = 5$ ; figure 8a). Although not statistically detectable, the variation in NKA activities of all ELISA samples is consistently low compared with those of the conventional methods, suggesting that the ELISA provides robust NKA quantification. Western blots of the recombinantly expressed NKA show that expression levels were even across biological replicates (electronic supplementary material, figure S2). This indicates that overall protein content is even within samples, and thus reduced variation in activity based on concentrations determined by the conventional methods would be expected.

Of note, activity measurements of the large milkweed bug NKA resulted in stark differences between the ELISA and conventional methods (figure 8b). The high activity associated with the conventional methods is due to them detecting very

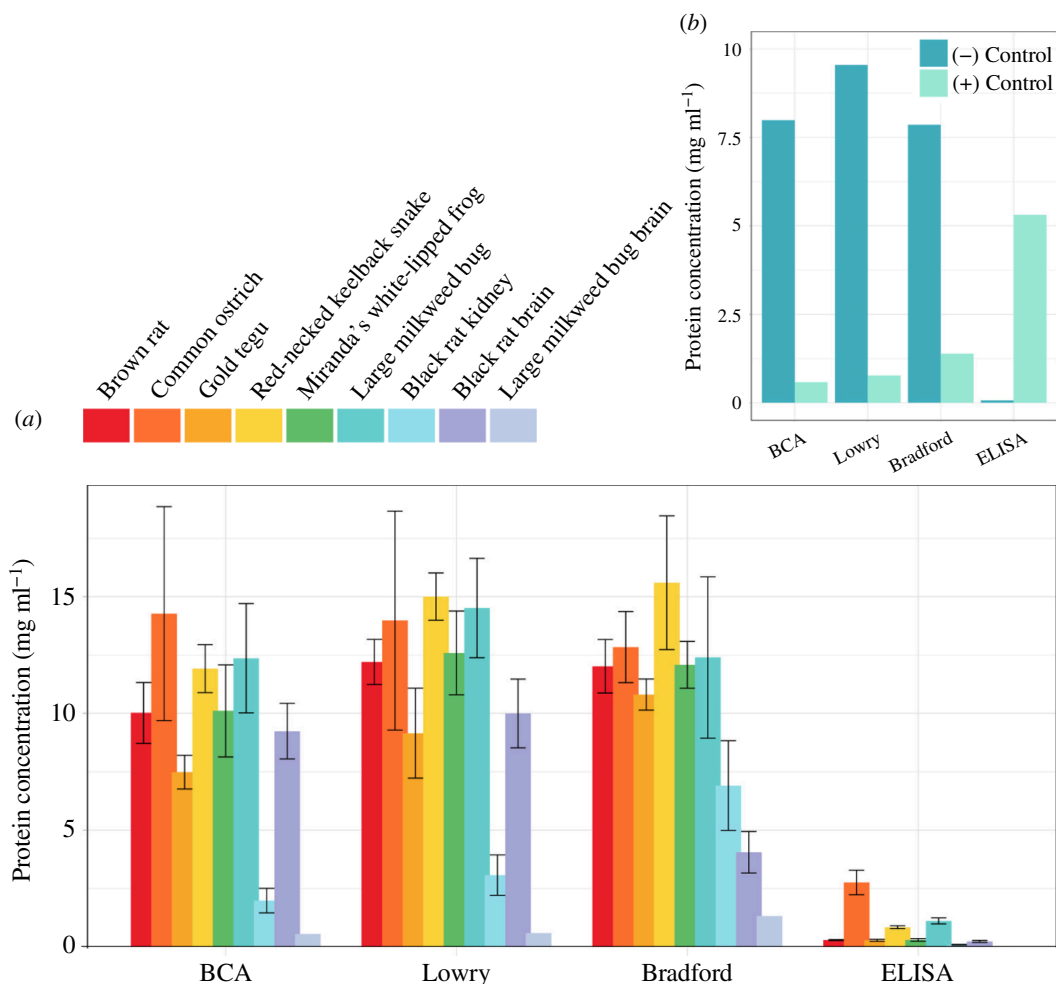


**Figure 6.** (a) Protein concentrations of recombinantly expressed and tissue-isolated NKAs. Bars represent the mean and standard error of three biological replicates, with the exception of Miranda's white-lipped frog and large milkweed bug brain, which consist of two and one replicates, respectively. (b) Protein concentrations of the negative control (membrane isolates of untransfected Sf9 cells) and positive control (commercial porcine NKA) determined by the four quantification methods reveals that the Lowry, BCA and Bradford cannot sufficiently detect NKA.

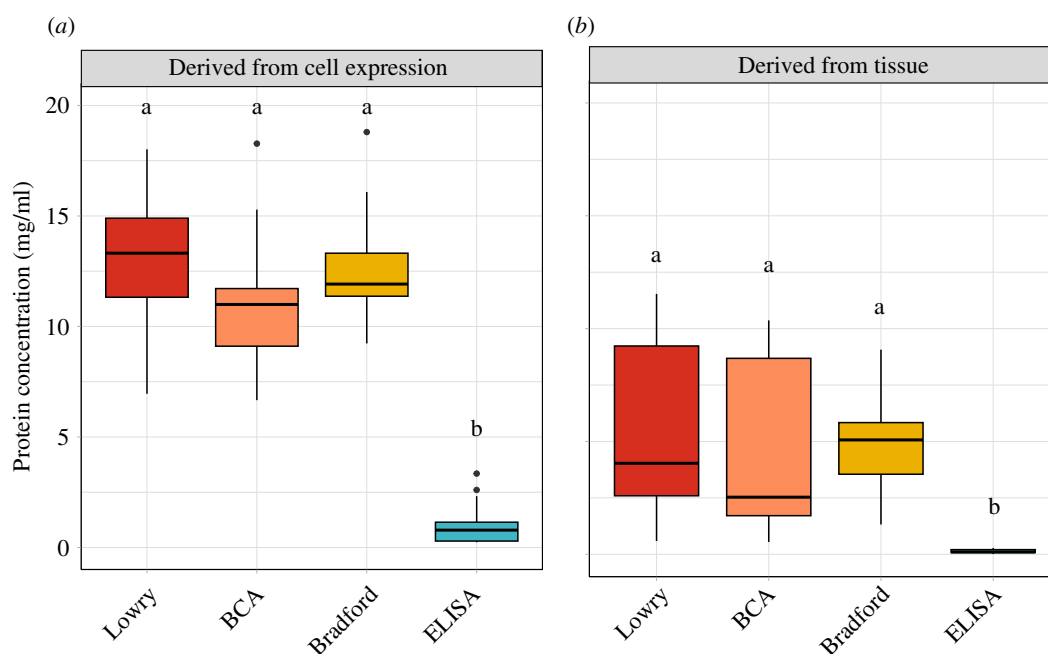


**Figure 7.** Comparison of protein concentrations determined by three conventional protein quantification methods and the ELISA from (a) recombinantly expressed NKA and (b) tissue-isolated proteins. Determined protein concentrations of different samples were pooled for each method. The boxes show the 25% and 75% quantiles of the median (thick line), the whiskers represent the maximum or minimum values without outliers. Outliers (filled-in circles) are protein concentrations greater or less than 1.5 times the interquartile range. Sample sizes for all four methods:  $n = 17$  (samples derived from Sf9 cells) and  $n = 9$  (nervous tissue and kidney isolates). Different letters indicate significant differences in the distribution of determined protein concentrations at  $p < 0.05$  (Dunn's test).



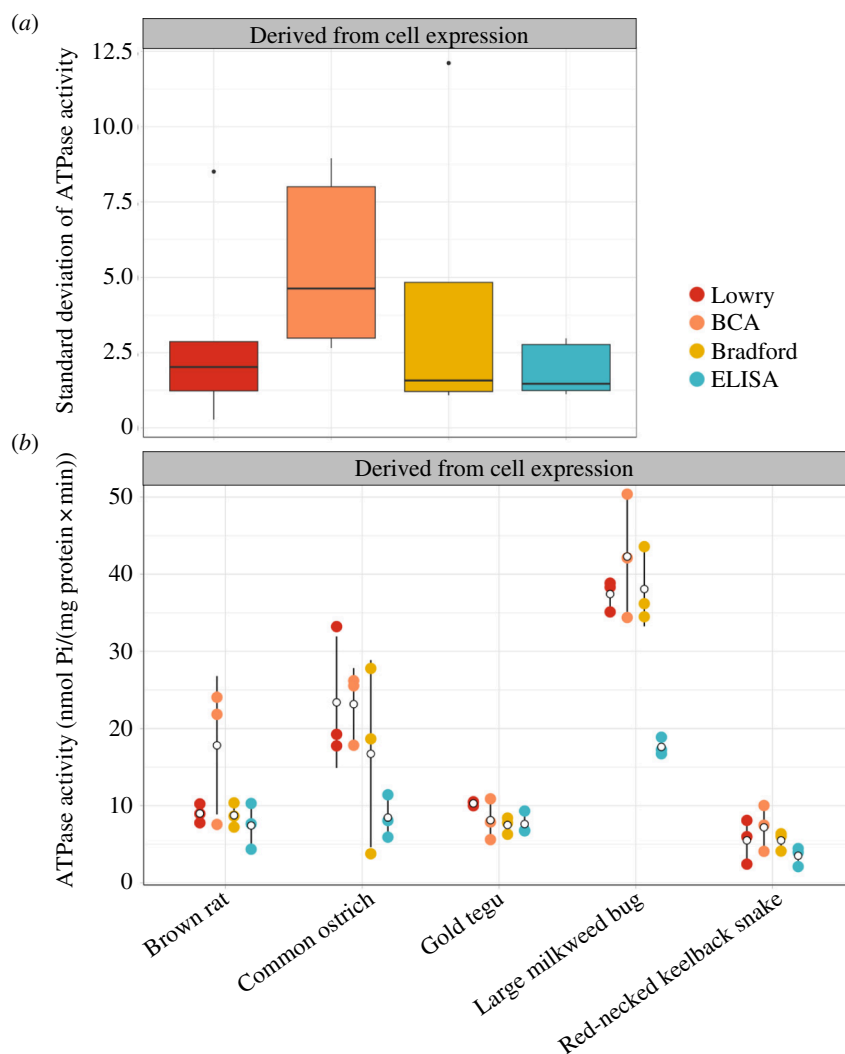


**Figure 8.** Comparison of the standard deviations (SDs) of Na, K-ATPase (NKA) ATPase activities measured based on protein concentrations determined by the four different protein quantification methods. (a) Pooled means showed no significant differences in SDs between the four methods. The box plots show the 25% and 75% quantiles of the median (thick line) and the maximum or minimum values without outliers (whiskers). Outliers (filled-in circles) are ATPase activities greater or less than 1.5 times the interquartile range. The sample size for each protein quantification method is  $n = 15$ . (b) Comparison of the variation in NKA activity of protein content calculated from concentrations determined by the four different protein quantification methods. Means and standard deviations of the three biological replicates are shown as hollow black circles and lines. Raw data points are shown as filled-in circles. Samples isolated from tissues were excluded from this analysis because activity levels fell beyond the linear range of standards.

low concentrations of the milkweed bug proteins, resulting in more protein being added to the activity assay reaction, and subsequently higher measured activity. By contrast, the ELISA detected rather high NKA concentrations in the large milkweed bug, which resulted in less protein being used for the activity assays, and thus lower activity measurements. This pattern can be seen across samples but is most pronounced in the milkweed bug.

By contrast to the Sf9-derived samples, the NKA activities of tissues-derived samples deviate from this pattern, showing high variation across all four quantification methods. Almost all the activity values of tissue samples fell far beyond the linear range of the  $P_i$  standard curve. Thus, we could not make accurate activity estimates for most of these samples. For this reason, they were excluded from the ANOVA analysis.

#### 4. Discussion

The overarching aim of this paper was to find a reliable method for quantifying large transmembrane proteins. We focused on the NKA as a model and we developed an ELISA that can be easily adapted across protein types and sources (i.e. species). We assessed the specificity of our ELISA in comparison with commonly used conventional quantification methods (Lowry, BCA and Bradford) and found that all conventional methods are generally unsuitable for quantifying NKA. Further, the concentration of the negative control, which consisted of untransfected Sf9 cells, determined by the conventional methods fell within the same range as transfected cells (figure 6b). These outcomes are a clear indication that the Lowry, BCA and Bradford assays have difficulty detecting transmembrane proteins. We would also point out that according to the SDS-PAGE, the  $\alpha$ -subunit content of membrane isolates is quite small compared with the overall protein content. This pattern is reflected in our results, with the ELISA-determined concentrations being significantly lower than the conventional methods. The high concentrations determined by the conventional methods are thus due to the high overall protein content of the samples.

There are several possible explanations for why the conventional quantification methods are inefficient at detecting transmembrane proteins. We rule out interfering substances, such as detergents, as a likely explanation for the inefficiency of the conventional methods because we used HPLC grade water for the resuspension of isolated proteins. We can also rule out glycosylation as a possible source of interference. Whereas glycosylation can lead to over- (Lowry and BCA) or underestimation (Bradford) of protein concentrations [35] and the NKA  $\beta$ -subunit is highly glycosylated, our results do not show under or over-estimation of proteins by the conventional methods—the high concentrations only occur in the heterogeneous samples, which rather reflect high background content.

The most likely explanation has to do with the fact that the main detection molecules of the conventional protein quantification methods, Coomassie brilliant blue and  $\text{Cu}^{2+}$ , are not able to penetrate the hydrophobic cell membrane [11]. Isolated transmembrane proteins are embedded in membrane fragments and therefore the embedded portion of the protein is not accessible to Coomassie brilliant blue and  $\text{Cu}^{2+}$  molecules, which bind to specific amino acids on the protein surface. This would consequently result in underestimated protein concentrations, and even more so considering that the protein standards for the conventional methods consist of non-membrane proteins. Although penetrating the cell membrane should be less of a barrier for the Lowry method because its alkaline reaction can disrupt cell membranes through hydrolysis, the results did not show higher detectability by this method compared with the other two (figures 6b and 7). By contrast, the  $\alpha 5$ -antibody of the ELISA binds to an epitope on the NKA  $\alpha$ -subunit located outside the cell membrane. Therefore, the detection pathway of the ELISA is not hindered by the membrane and the resulting concentration measurement reflects a reliable estimate of the number of NKA molecules in the sample. A possible alternative would be to produce the relative standards as described for our ELISA and use them in conjunction with one of the conventional methods. However, we doubt that a reliable standard curve can be obtained with transmembrane proteins.

One unexpected outcome of these experiments is that all quantification methods detected lower protein concentrations in the tissue-derived samples compared with the recombinantly expressed Sf9 cell-derived samples. It is possible that the lowered detection of proteins in tissue samples is due to differences in the membrane composition, or co- and post-transcriptional modifications of Sf9 cells and tissue cells, which might alter the accessibility of the epitope to the primary  $\alpha 5$ -antibody. In this case, the tissue sample concentrations would also be lowered as a result of using relative standard curves produced from Sf9 cell-derived NKA. The stark difference in detectability of rat NKA derived from recombinantly expressed Sf9 cells and from kidney tissue, both of which consist of the rat isoform  $\alpha 1$  (ATP1A1), supports this hypothesis.

The NKA activity assays, which were run based on protein concentrations determined by the different quantification methods, helped to serve as an additional robustness assessment of the methods. The activity data of Sf9 cell-derived NKA showed consistently low variation across all animal species when the NKA activity assays were based on ELISA-determined protein concentrations (figure 8). The NKA activity assays based on concentrations determined by the three conventional methods exhibited different levels of variation across animal species—meaning that some animal species exhibited low variation in NKA activities while others exhibited high variation (figure 8). Due to these overlaps, it was not possible to detect a statistical difference between NKA activity variation in ELISA-based and other quantification method-based data. According to the ELISA, the determined NKA concentrations of protein samples derived from Sf9 cells were quite similar across the three biological replicates of each animal species. The conventional methods determined protein concentrations that were considerably lower, but, as with ELISA, they differ only slightly across biological replicates. This, in turn, resulted in lower variation in NKA activities for the conventional methods. The even NKA expression across biological replicates, as seen on the western blots (electronic supplementary material, figure S2), further corroborate why no statistical difference was detected in the NKA activity variation between the four protein quantification methods. If NKA expression levels were uneven across biological replicates, then we would have expected to see more variation in the resulting activity data based on the conventional methods.

Of note, we found that the NKA activity assays of tissue-derived samples exhibited very high variation across the board. This was probably due to the absorbance values measured for the activity assays exceeding the linear range of the  $\text{P}_i$  standard curve, making accurate quantification of phosphate released from the hydrolysis of ATP impossible. There are two possible explanations for this outcome. The first is that NKAs derived from tissue have a higher catalytic activity than those expressed recombinantly. When the NKA activity is very high, then considerably less protein would be needed in the NKA activity assay to fall within the detectable range of the standard curve. Another explanation is that all four quantification methods, including the ELISA, severely underestimated the total NKA concentrations in tissue-derived samples, as was discussed previously. When the NKA concentration is underestimated, then more protein is used in the NKA activity assay, driving the NKA activity levels beyond the linear range of the standard curve. Despite numerous rounds of dilutions, we were never able to capture activity levels that fell within the standards range for our tissue-derived samples.

As part of the functional validation of the ELISA, several negative controls were run to test non-specific background noise in the ELISA. The negative control containing only NKA and the secondary HRP-antibody ('no  $\alpha 5$ -antibody') showed a slightly higher absorbance than the detection threshold (figure 5). This minimal background noise probably results from HRP-antibodies that remain in the wells after washing. For this reason, the number of wash steps following HRP-antibody incubation is higher than the rest of the washing steps. The absorbances of the other negative controls containing no HRP-conjugated secondary antibody or no protein sample did not exceed the detection threshold, indicating that TMB and the stopping solution do not stain non-specifically and that non-specific binding of the antibodies to the wells is not an issue in this ELISA.

Another important validation step involved confirming by western blot and ELISA that lyophilization does not alter the detectability of NKA by the antibodies used in the ELISA, thereby ensuring that the standards will not be detected differently than the fresh protein samples. Verifying that lyophilized cell membrane isolates can be used to produce relative protein standards is important considering how different the relative NKA standard curves can look for different animal species (figure

4). Without producing a standard curve for each animal species, the determined NKA concentrations would be biased towards the detectability of the protein's animal species origin and thus significantly over- or underestimate NKA content in different samples. These interspecies differences are due to the  $\alpha 5$ -antibody binding at different efficiencies with different animal species (figure 4; electronic supplementary material, figure S3).

Overall, our results indicate that the ELISA is the most suitable quantification method for the NKA, and most likely other large transmembrane proteins as well. The ELISA validated here can be easily adapted to other transmembrane proteins by exchanging the primary and, if necessary, the secondary antibody. Moreover, it is straightforward to prepare relative protein standards that can be adapted to a wide taxonomic range and multiple sample types. This method eliminates the need for commercially available ELISA kits, which are more limited in these regards and can be quite costly.

**Ethics.** This work did not require ethical approval from a human subject or animal welfare committee.

**Data accessibility.** All data produced in this paper are accessible in the supplementary materials [36].

**Declaration of AI use.** We have not used AI-assisted technologies in creating this article.

**Authors' contributions.** J.L.: conceptualization, formal analysis, investigation, methodology, resources, visualization, writing—original draft, writing—review and editing; S.V.: data curation, formal analysis, investigation, methodology, validation, visualization, writing—original draft, writing—review and editing; S.D.: conceptualization, project administration, supervision, writing—review and editing; S.M.: conceptualization, project administration, supervision, writing—original draft, writing—review and editing.

All authors gave final approval for publication and agreed to be held accountable for the work performed therein.

**Conflict of interest declaration.** We declare we have no competing interests.

**Funding.** This study was supported by grants to S.D. from the Deutsche Forschungsgemeinschaft (Do 517/10-1) and to S.M. from the Alexander von Humboldt Foundation (Mohammadi 2018) and the National Institutes of Health (F32-HL149172).

**Acknowledgements.** We thank M. Hertz and V. Wagschal for their assistance in the laboratory. We also thank the anonymous reviewer(s) who put a great deal of effort into providing constructive feedback and suggestions that significantly improved this paper.

## References

- Mohammadi S, Herrera-Álvarez S, Yang L, Rodríguez-Ordoñez MDP, Zhang K, Storz JF, Dobler S, Crawford AJ, Andolfatto P. 2022 Constraints on the evolution of toxin-resistant Na, K-ATPases have limited dependence on sequence divergence. *PLoS Genet.* **18**, e1010323. (doi:10.1371/journal.pgen.1010323)
- Dalla S, Baum M, Dobler S. 2017 Substitutions in the cardenolide binding site and interaction of subunits affect kinetics besides cardenolide sensitivity of insect Na, K-ATPase. *Insect Biochem. Mol. Biol.* **89**, 43–50. (doi:10.1016/j.ibmb.2017.08.005)
- Orlowski J, Lingrel JB. 1988 Tissue-specific and developmental regulation of rat Na, K-ATPase catalytic alpha isoform and beta subunit mRNAs. *J. Biol. Chem.* **263**, 10436–10442.
- Ahrens HE *et al.* 2015 siRNA mediated knockdown of tissue factor expression in pigs for xenotransplantation. *Am. J. Transplant.* **15**, 1407–1414. (doi:10.1111/ajt.13120)
- Lowry OH, Rosebrough NJ, Farr AL, Randall RJ. 1951 Protein measurement with the Folin phenol reagent. *J. Biol. Chem.* **193**, 265–275.
- Smith PK *et al.* 1985 Measurement of protein using bicinchoninic acid. *Anal. Biochem.* **150**, 76–85. (doi:10.1016/0003-2697(85)90442-7)
- Bradford MM. 1976 A rapid and sensitive method for the quantitation of microgram quantities of protein utilizing the principle of protein-dye binding. *Anal. Biochem.* **72**, 248–254. (doi:10.1016/0003-2697(76)90527-3)
- Fanger BO. 1987 Adaptation of the Bradford protein assay to membrane-bound proteins by solubilizing in glucopyranoside detergents. *Anal. Biochem.* **162**, 11–17. (doi:10.1016/0003-2697(87)90004-2)
- Mehl JW, Pacovska E, Winzler RJ. 1949 The amount of copper bound by protein in the biuret reaction. *J. Biol. Chem.* **177**, 13–21. (doi:10.1016/S0021-9258(18)57051-4)
- Friedenauer S, Berlet HH. 1989 Sensitivity and variability of the Bradford protein assay in the presence of detergents. *Anal. Biochem.* **178**, 263–268. (doi:10.1016/0003-2697(89)90636-2)
- Kirazov LP, Venkov LG, Kirazov EP. 1993 Comparison of the lowry and the Bradford protein assays as applied for protein estimation of membrane-containing fractions. *Anal. Biochem.* **208**, 44–48. (doi:10.1006/abio.1993.1006)
- Cienfuegos-Jiménez O, Morales-Hernández A, Robles-Rodríguez OA, Bustos-Montes S, Bañuelos-Alduncin KA, Cortés-Castillo AR, Barreto-Hurtado HD, Carrete-Salgado L, Marino-Martínez IA. 2022 High-yield production and purification of the fusion pH-responsive peptide GST-pHLIP in *Escherichia coli* BL21. *AIMS Mol. Sci.* **9**, 136–144. (doi:10.3934/molsci.2022008)
- Yadavalli R, Sam-Yellowe T. 2015 HeLa based cell free expression systems for expression of plasmodium rhoptry proteins. *J. Vis. Exp.* e52772. (doi:10.3791/52772)
- Dobler S, Wagschal V, Pietsch N, Dahdoui N, Meinzer F, Romey-Glusing R, Schütte K. 2019 New ways to acquire resistance: imperfect convergence in insect adaptations to a potent plant toxin. *Proc. R. Soc. B* **286**, 20190883. (doi:10.1098/rspb.2019.0883)
- Karageorgi M *et al.* 2019 Genome editing retraces the evolution of toxin resistance in the monarch butterfly. *Nature* **574**, 409–412. (doi:10.1038/s41586-019-1610-8)
- Mohammadi S *et al.* 2021 Concerted evolution reveals co-adapted amino acid substitutions in Na<sup>+</sup>K<sup>+</sup>-ATPase of frogs that prey on toxic toads. *Curr. Biol.* **31**, 2530–2538. (doi:10.1016/j.cub.2021.03.089)
- Engvall E, Perlmann P. 1972 Enzyme-linked immunosorbent assay, Elisa. III. Quantitation of specific antibodies by enzyme-labeled anti-immunoglobulin in antigen-coated tubes. *J. Immunol.* **109**, 129–135. (doi:10.4049/jimmunol.109.1.129)
- Gan SD, Patel KR. 2013 Enzyme immunoassay and enzyme-linked immunosorbent assay. *J. Invest. Dermatol.* **133**, 1–3. (doi:10.1038/jid.2013.287)
- Kaplan JH. 2002 Biochemistry of Na, K-ATPase. *Annu. Rev. Biochem.* **71**, 511–535. (doi:10.1146/annurev.biochem.71.102201.141218)
- Scheiner-Bobis G. 2002 The sodium pump. Its molecular properties and mechanics of ion transport. *Eur. J. Biochem.* **269**, 2424–2433. (doi:10.1046/j.1432-1033.2002.02909.x)
- Hertz M, Dalla S, Wagschal V, Turjalei R, Heiser M, Dobler S. 2024 Coevolutionary escalation led to differentially adapted paralogs of an insect's Na, K-ATPase optimizing resistance to host plant toxins. *Mol. Ecol.* **33**, e17041. (doi:10.1111/mec.17041)
- Blanco G, Xie ZJ, Mercer RW. 1993 Functional expression of the alpha 2 and alpha 3 isoforms of the Na, K-ATPase in baculovirus-infected insect cells. *Proc. Natl Acad. Sci. USA* **90**, 1824–1828. (doi:10.1073/pnas.90.5.1824)
- DeTomaso AW, Xie ZJ, Liu G, Mercer RW. 1993 Expression, targeting, and assembly of functional Na, K-ATPase polypeptides in baculovirus-infected insect cells. *J. Biol. Chem.* **268**, 1470–1478. (doi:10.1016/S0021-9258(18)54099-0)

24. Scholz J, Suppmann S. 2017 A new single-step protocol for rapid baculovirus-driven protein production in insect cells. *BMC Biotechnol.* **17**, 83. (doi:10.1186/s12896-017-0400-3)
25. Herbertz M, Harder S, Schlüter H, Lohr C, Dobler S. 2022 Na, K-ATPase  $\alpha$ 1 and  $\beta$ -subunits show distinct localizations in the nervous tissue of the large milkweed bug. *Cell Tissue Res.* **388**, 503–519. (doi:10.1007/s00441-022-03580-6)
26. Lohr JN, Meinzer F, Dalla S, Romey-Glüsing R, Dobler S. 2017 The function and evolutionary significance of a triplicated Na, K-ATPase gene in a toxin-specialized insect. *BMC Evol. Biol.* **17**, 256. (doi:10.1186/s12862-017-1097-6)
27. Yu Y *et al.* 2014 A rat RNA-Seq transcriptomic BodyMap across 11 organs and 4 developmental stages. *Nat. Commun.* **5**, 3230. (doi:10.1038/ncomms4230)
28. Yue F *et al.* 2014 A comparative encyclopedia of DNA elements in the mouse genome. *Nature* **515**, 355–364. (doi:10.1038/nature13992)
29. Djamgoz MBA, Ready PD, Billingsley PF, Emery AM. 1998 Insect Na(+)/K(+)-ATPase. *J. Insect Physiol.* **44**, 197–210. (doi:10.1016/s0022-1910(97)00168-6)
30. Fedosov SN, Nexo E, Heegaard CW, Goldin J, Mason JB. 2023 Protein binding assays for an accurate differentiation of vitamin B12 from its inactive analogue: a study on edible cricket powder. *Food Chem.* **19**, 100824. (doi:10.1016/j.fochx.2023.100824)
31. Petschenka G, Fandrich S, Sander N, Wagschal V, Boppré M, Dobler S. 2013 Stepwise evolution of resistance to toxic cardenolides via genetic substitutions in the Na+/K+ -ATPase of milkweed butterflies (Lepidoptera: Danaini). *Evolution* **67**, 2753–2761. (doi:10.1111/evo.12152)
32. Taussky HH, Shorr E. 1953 A microcolorimetric method for the determination of inorganic phosphorus. *J. Biol. Chem.* **202**, 675–685.
33. Schneider CA, Rasband WS, Eliceiri KW. 2012 NIH Image to ImageJ: 25 years of image analysis. *Nat. Methods.* **9**, 671–675. (doi:10.1038/nmeth.2089)
34. Kassambara A. 2023 Rstatix: pipe-friendly framework for basic statistical tests, version 0.7.2. See <https://cran.r-project.org/web/packages/rstatix/index.html>.
35. Fountoulakis M, Juranville JF, Manneberg M. 1992 Comparison of the Coomassie brilliant blue, bicinchoninic acid and Lowry quantitation assays, using non-glycosylated and glycosylated proteins. *J. Biochem. Biophys. Methods* **24**, 265–274. (doi:10.1016/0165-022x(94)90078-7)
36. Löptien J, Vesting S, Dobler S, Mohammadi S. 2024 Supplementary material from: Evaluating the efficacy of protein quantification methods on membrane proteins. Figshare. (doi:10.6084/m9.figshare.c.7547683)